UNCLASSIFIED

Research Report No. 126

UNIVERSITY OF MINNESOTA
INSTITUTE OF TECHNOLOGY
DEPARTMENT OF AERONAUTICAL ENGINEERING
ROSEMOUNT AERONAUTICAL LABORATORIES

easurement of Recovery Factors and Heat Transfer Coefficients with anspiration Cooling in a Turbulent oundary Layer at M=3 Using Air and Helium as Coolants

by
B. M. Leadon and C. J. Scott

A Research Program for the
United States Air Force
Air Research and Development Command
Contract AF 18 (600)-1226

Minneapolis 14, Minnesota
February 1956

Research Report No. 126 Copy No. 10

UNIVERSITY OF MINNESOTA
INSTITUTE OF TECHNOLOGY
DEPARTMENT OF AERONAUTICAL ENGINEERING
ROSEMOUNT AERONAUTICAL LABORATORIES

MEASUREMENT OF RECOVERY FACTORS AND HEAT TRANSFER COEFFICIENTS WITH TRANSPIRATION COOLING IN A TURBULENT BOUNDARY LAYER AT M = 3.0 USING AIR AND HELIUM AS COOLANTS

by

B. M. Leadon and C. J. Scott

FC

Prepared for United States Air Force
Office of Scientific Research
Air Research and Development Command
Contract AF 18 (600)-1226

Minneapolis 14, Minnesota
February 1956

APPROVED John D. Akerman
John D. Akerman
Head of Dept. and Director of
Rosemount Aero. Laboratories

BIBLIOGRAPHICAL CONTROL SHEET

1. Originating agency and monitoring agency:
   O.A.: University of Minnesota, Rosemount Aeronautical Laboratories
   Rosemount, Minnesota
   M.A.: Fluid Mechanics Division, Office of Scientific Research

2. Originating agency and monitoring agency report number:
   O.A.: RAL Research Report No. 126
   M.A.: AFOSR-TN-56-94

3. Title and classification of title:
   MEASUREMENT OF RECOVERY FACTORS AND HEAT TRANSFER COEFFICIENTS WITH TRANSPIRATION COOLING IN A TURBULENT BOUNDARY LAYER AT M = 3 USING AIR AND HELIUM AS COOLANTS (UNCLASSIFIED)

4. Personal authors: B. M. Leadon and C. J. Scott

5. Date of report: February 1956

6. Pages: 36 pages

7. Illustrative material: 12 figures

8. Prepared for Contract No.: AF 18 (600)-1226

9. Prepared for Project No.: R-352-50-4

10. Security Classification: UNCLASSIFIED

11. Distribution limitations: None

12. Abstract: Turbulent recovery factor and heat transfer measurements have been made on a porous wall section at a nominal Mach number of 3.0 and a Reynolds number of approximately 4×10^6 using both air and helium as the transpired gas. Measured heat transfer coefficients correlate well with the compressible theory of Rubesin[2] for air and qualitatively with simple film theory for either coolant, indicating that the heat transfer from a turbulent boundary layer can be reduced by transpiration cooling to well below that of the uncooled boundary layer at the same Reynolds number.

    The simple film theory[1] is extended to apply to binary boundary layers with any concentration of foreign gas at the wall.

FOREWORD

This report was prepared by the Department of Aeronautical Engineering of the University of Minnesota, under the direction of Dr. B. M. Leadon. The investigation was conducted under USAF Contract AF 18 (600)-1226 and was administered under the direction of the Office of Scientific Research with Mr. E. Haynes acting as Project Engineer.

Administration of the contract at the University of Minnesota was provided by Professor John D. Akerman, Head of Department and Mr. Richard V. DeLeo, Administrative Scientist.

Included among those who cooperated in the study at the Rosemount Aeronautical Laboratories of the University of Minnesota were M. D. Pearson, D. C. Friedman, C. M. Overby and G. E. Anderson.

INTRODUCTION

Viscous dissipation of energy in the boundary layer reaches such magnitude and the layer is so thin in the case of supersonic aircraft that it becomes exceedingly difficult to maintain a moderate surface temperature by means of internal cooling. Heat transfer rates are even greater if the boundary layer state is turbulent instead of laminar. It becomes of interest therefore to study other means of cooling the surfaces of high speed aircraft and as an idealization to study the cooling of a flat plate aligned with the flow.

These considerations lead one to separate studies of laminar and turbulent boundary layers and of transition as affected by the introduction of liquids and light gases directly into the boundary layer itself. The coolants may be injected into the outer flow either at well-separated locations or almost continuously by means of closely spaced pores. Since transition to turbulence will be promoted by the "roughness" of the injection mechanism, it is conservative at first to assume that transpiration cooling will be concurrent with a turbulent boundary layer state.

When the usual solid wall boundary condition of zero normal velocity is replaced, for a porous wall, by one of finite normal velocities, it is to be expected that the properties of the viscous boundary layer associated with a convective flow over the wall will be affected. The distributions normal to the surface of such descriptive variables as velocity, temperature, and concentration of foreign gas may be modified strongly if gas is intro-

duced which has markedly different kinetic and thermal properties from those of the free stream gas. Of practical interest are two possibilities: (1) the rate of heat transfer to the wall may be reduced to a significant extent by a small mass flow of transpired gas, and (2) the laminar stability of the boundary layer may be improved. Experiments on the first possibility for a turbulent boundary layer in a supersonic flow are reported herein.

Theories have been presented for statistically steady turbulent boundary layer flow including the effect of finite normal velocity at the wall. Film theory[1] involves such crude assumptions that it may be accepted only qualitatively, but it displays the effect of mass diffusion in a simple manner whereas the more refined analytical estimates based upon mixing-length theory[2,3] are available at present only for the case of air blowing into air.

Reference 1 presents a summary of the experimental and theoretical work done in the field of transpiration cooling prior to July 1954.

THEORY

Analytical estimates of the effect of porous wall injection directly into a turbulent boundary layer are available in the reports of Rubesin[2] and of Dorrance and Dore[3], but neither of these treats a coolant gas having properties different from those of air. Both are based upon classical mixing length theory, and both are rather tedious to work out. Consequently, only the former is calculated for conditions of the present experiment, but it is understood that the two analyses are in general agreement[2,4].

A highly simplified theory is presented by Mickley, Ross, Squyers and Stewart[1] for binary boundary layers whose concentration of foreign gas is equal to unity at the wall. This film theory is reconsidered in Appendix A of this report and is extended to pertain to any wall concentration.

EXPERIMENTAL APPARATUS

The test setup is shown in a general view in Fig. 1. A 7 x 1.5-inch porous flat plate constructed of sintered stainless steel wire was set into the straight wall in the constant pressure section of a 1.9 x 1.75 inch, asymmetric, supersonic channel with its leading edge located 7.5 inches from the throat. The nozzle block, made of a fiberglass laminate having low thermal conductivity (Scotchply), was machined to contain a coolant stilling chamber. Thermocouples, 0.0031 in. diam., were carefully installed in the porous surface and suspended throughout the coolant stilling chamber at one inch intervals. Provision was made to heat the porous surface electrically and to preheat the injected gas.

SUPERSONIC CHANNEL

The instrumentation wind tunnel has a 1.75 by 1.9 inch test section which operates continuously at a nominal Mach number of 3 over a local Reynolds number per inch range of 0.14×10^6, 2.1×10^6. The air is dried to an average dew point of -40°F. The nozzle is asymmetric, consisting of a flat lower block and a contoured upper block, both fabricated from a laminate consisting of resin plastic reinforced with linearly aligned glass filaments and called "Scotchply" by Minnesota

Mining and Manufacturing Company. A photograph of the test section with one side-plate removed is shown as Fig. 2. The lower block serves as the test wall to take advantage of the apex of the test rhombus. The actual Mach number distribution along the straight wall was surveyed for these tests (Fig. 3). The porous surface is installed in the wall space between stations 7-3/4 and 14-1/2 inches downstream of the throat. In order to distribute the incoming coolant well, a plenum chamber, enclosing a porous bronze baffle plate, was cut in the nozzle block (Fig. 4).

POROUS FLAT PLATE

Samples of sintered woven wire, sintered powder, perforated plate and wire screen were tested for permeability in terms of mass flux of air versus a pressure drop parameter defined as the average pressure times the pressure gradient through the material (Fig. 5). 1-1/2 inch diameter samples were tested in a sealed duct with controlled pressure and vacuum reservoirs connected to the opposite ends. The results showed that both sintered powder and sintered woven wire are manufactured in a wide range of permeabilities.

The test material used in the model was a flat plate of sintered stainless steel wire (Poroloy, Pacoima, Calif.). It was selected because a sample at hand (t = .050") provided a sufficient pressure drop for uniform flow distribution (sample 1, Fig. 5), and also it has practical interest because of its tensile strength. The surface appeared aerodynamically rough - the roughness was apparent to the touch - as may be seen in Fig. 6.

The coolant was blocked by a support shelf milled in the nozzle surface 1/8" wide all around the edge and by the copper bars soldered to each end. Thus, the actual blowing area was 6.1 x 1.25 inches. The last inch of the porous plate was not used in calculating local heat transfer coefficients because of the free stream pressure gradient near the rear of the plate. Also, the first inch of the plate was not used because of the local temperature gradient (Fig. 8).

THERMOCOUPLE INSTALLATION

After investigation of the attendent problems, the technique of heating the porous surface electrically was chosen. The only serious restriction imposed by this method is that heat flows must always be from the surface outward to the free stream.

Through the use of preheating, the temperature of the "coolant" gas can be brought into equilibrium with the surface temperature. Thus, allowing for small surface temperature variations, it is possible to hold a small temperature difference between any point on the test surface and the coolant supply chamber. This being true, conduction errors are small even for leads brought straight through the porous surface. In this arrangement the disturbance to the uniform porosity of the surface caused by inserting the solid wires and insulation is minimized.

In an effort to further reduce the conduction errors, iron-constantan thermocouples were used because of their relatively low conductivity, and 40 gauge wire (d = .0031 inch) because of its small cross-sectional area. Blockage was held down by taking pains to achieve a neat

installation. A 0.013 inch diameter hole was drilled through the surface and a cylindrical teflon plug was pressed into the hole, a 0.003 inch diameter hole was drilled in the teflon plug and the thermocouple lead was pressed through it. The thermocouple lead was spot welded to the porous surface. That the area blocked by the thermocouple installation was almost negligible may be seen in Fig. 6. The Teflon insulation passed partially through the surface wires and never completely blocked any pore. Microscopic inspection revealed that the insertion of the thermocouple lead wires and the welding of the ends to the surface wires did not seriously impair the local porosity. The roughness of the thermocouple installation was comparable to the surface roughness of the wire mesh.

Six iron-constantan thermocouples, Fig. 6, were spot welded to the outer surface at one inch intervals along the center line in the plate, and connected to a thermocouple selector switch. The iron lead which formed one side of each iron-constantan thermocouple was used as a voltage tap. Thus, nearly simultaneous readings of voltage increment and surface temperature were obtainable.

ELECTRICAL HEATING SYSTEM

The stainless steel sintered wire porous test plate served as the resistance element of a high-amperage, 60-cycle alternating current electrical circuit. Copper bus-bars were silver soldered to the front and rear edges of the test plate.

The bus bars were supplied through a voltage regulator and step-down transformer from a 115-volt a.c. line (Fig. 4). Current was measured using a current transformer and voltage drop was measured locally with an electronic voltmeter.

COOLANT SYSTEM

The complete coolant system requires a foreign gas reservoir, mass flow regulation, and surface temperature control. Both compressed air and helium were available to serve as the coolant gas. A 22-bottle helium manifold, containing 4400 standard cubic feet at approximately 2200 psi, served as the helium supply. A pressure regulator and calibrated sonic orifices were used to regulate and measure the mass flow. The orifice areas were calibrated by measuring the pressure versus time curve of the flow into a evacuated tank of known volume. The orifices, connected in parallel, provided a maximum to minimum mass flow ratio of 100.

The heater and cooler were connected in parallel to provide a means of temperature control (Fig. 7). The heater consisted of two concentric stainless steel cylinders which are closed at each end. A 4-inch diameter porous sintered bronze plug containing 7-100 watt heating rods was cemented inside the inner chamber. This unit takes advantage of the larger surface area in the porous bronze to provide a higher heating efficiency. The pressure level between the concentric cylinders was reduced to less than 0.05 psia to reduce the heat conducted away from the heater cylinder.

The cooler consisted of two chambers connected by nine 1-inch copper tubes. A six-inch length of porous sintered bronze was soldered inside each of the copper tubes. The complete cooler assembly was submerged in a bath of dry ice and alcohol (-109.8°F).

POROUS SURFACE HEAT BALANCE

A heat balance on a segment of the porous surface results in the equation governing the present experiment:

$$h(T_w - T_{aw}) = (\rho v c_p)_c (T_c - T_w) + q_E - q_{rad} - q_{losses} \qquad (1)$$

where symbols denote

- h, heat transfer coefficient,
- T, temperature,
- ρ, density,
- v, normal velocity
- c_p, specific heat at constant pressure,
- q, heat flux,

and subscripts refer to

- w, wall value
- aw, recovery value (adiabatic wall value),
- c, coolant value
- E, due to electrical heating,
- rad, due to radiant cooling
- losses, due to extraneous conduction losses,

respectively.

In addition we define Stanton number here as

$$St = \frac{h}{\rho_{\infty} U_{\infty} C_{p_{\infty}}} \qquad (2)$$

where subscript ∞ refers to free stream values.

EXPERIMENTAL TECHNIQUE

The data was taken on two separate days. During the first day various exploratory runs were made, and on the second day the data was taken more systematically. The results from the two days correlated very well which indicated that systematic errors due to technique were small. For example, the zero blowing heat transfer rates showed a scatter of $\pm$ 5%.

The basic experimental procedure employed was as follows. Supersonic flow was established in the wind tunnel and the tunnel pressure was adjusted to the proper free stream Reynolds number per inch. The desired coolant flow was established and the nozzle block preheated to the same temperature as the coolant gas for approximately one-half hour prior to any data taking. Once the nozzle block was at a uniform desired temperature, the temperature of the coolant was stabilized at approximately 135°F and the electrical energy to the surface was adjusted until the surface temperature equalled the coolant temperature at one longitudinal station. The system was allowed to stabilize, readjusting the flow and temperature conditions when necessary. A minimum of one-half hour was required to obtain steady state operation. Local values of voltage increment, surface temperature, and coolant temperature were measured at six longitudinal stations. The measurements, together with the current measurements, permitted direct evaluation of local heat flow rate.

A total of ten hours running time was consumed for the data presented. A typical surface temperature distribution along the porous section during the heated runs is shown as Fig. 8. The powers required to maintain an average surface temperature at 135°F with the injection of air and helium as coolants is shown as Fig. 9.

All data was taken at one tunnel Reynolds number per inch. The variation of Reynolds number over the points involved was $\pm$ 30% of which the mean was 3.8×10^6 based on the distance from the channel throat.

RECOVERY FACTOR MEASUREMENTS

In order to evaluate the local Stanton numbers as defined in Eq's. 1 - 2, it was necessary to measure local recovery temperatures. The recovery temperature, in this case defined by Equation (1), occurs when the surface temperature is equal to the coolant temperature. Exploratory runs showed the scatter to be due largely to variations in tunnel stagnation temperature. During data runs the tunnel T_o was held constant by controlling the output of the compressor so that no pressure change occurred in the storage tanks. Runs were made with no surface electrical heating. The nozzle block was precooled for one-half hour before the runs commenced by passing the coolant through the surface at the estimated recovery temperature. During the runs the coolant temperature was set at a level close to the estimated value. $T_w - T_c$ were recorded. Several coolant temperatures were set and a plot $T_w - T_c$ vs. T_w/T_o (Fig. 10) used to interpolate the value of the recovery temperature ($T_w = T_{aw}$ when $T_c = T_w$). Each value of local recovery factor

required a minimum of three separate runs. The results are shown in Fig. 11. The temperature distribution at local recovery temperature are plotted in Fig. 8. The zero blowing value of recovery factor was found to be $r_{0_t} = .9127$, which is somewhat higher than other published results (mainly on smooth models). Considerable deviation between thermocouples, as indicated by the flags as in Fig. 11, is in evidence and is felt to be due to surface temperature gradients, nonuniform coolant injection, and small errors in temperature difference measurements. Also observable is a slight decrease in recovery factor with Reynolds number since the flags at the upper right hand of the symbol represent the lowest Reynolds number and increasing Reynolds numbers are shown by rotating the flag counter-clockwise. The precision required in measuring $T_w - T_c$ to determine recovery temperature accurately at the higher blowing rates may be seen in Fig. 10. The fact that the trends are relatively consistent indicates the deviations are systematic and perhaps removable. This data was also checked by making runs on two separate days.

Curves were faired by eye through the recovery data. These curves were used to compute recovery temperatures in reducing the heat flow data to Stanton number plots.

RADIATION CORRECTION

Data on the emissivity of porous surfaces is generally unavailable at present, but the physical structure of the surface is such that its emissivity is relatively large. Calculations of the radiation per unit time and unit area from/to its surroundings indicated that the radiation

term was sizeable and subject to measurement.

The normal emissivity of the porous surface and of the opposing nozzle block was measured. A total radiation pyrometer was used together with an appropriate black body reference and suitable heaters and temperature recorders necessary to obtain experimental values of normal emissivity. At least two readings for each material were obtained giving the following average values:

Material	e_n	T-°F
Stainless steel Poroloy	.44	138
Scotchply plastic	.94	122

The radiant heat flow from a heated surface (w) in the wind tunnel (t) was computed from the following equation:

$$q_r = F_{12}\, e_{12}\, \sigma (T_w^4 - T_t^4)$$

where

F_{12} = function of radiation geometry

e_{12} = effective emissivity or interchange factor (for parallel infinite walls $\frac{1}{e_{12}} = \frac{1}{e_1} + \frac{1}{e_2} - 1 = \frac{1}{.42} - 1$ and for "small" surfaces $e_{12} = e_1 e_2 = .42$)

σ = 0.173 x 10^{-8} Btu/hr ft^2°R4, Boltzmann constant.

F_{12} was assumed to equal unity. The temperature of the wind tunnel nozzle block was assumed to be at the theoretical turbulent recovery temperature. Radiant heat flows computed from this equation were found to vary from 15 to 150 percent of the forced convection heat rates. Large radiation corrections were necessary when the convective heat rates had been greatly reduced by transpiration cooling.

UNIFORMITY OF INJECTION VELOCITY OF COOLANT

A single traverse of the nearly uniform coolant flow distribution behind the porous surface was conducted to evaluate the injected mass flow distribution. Only a partial survey, the rear 4 inches of the test piece, was possible using present equipment - an "Alnor" type 8500 thermo-anemometer. The traverse was carried out 3/4 inch below the test surface. An attempt to re-evaluate the recovery temperature data using the local mass flow rates determined slightly reduced the scatter of the recovery data. However, the need for a more efficient baffling system was made clear.

RESULTS

The combined results of the previously described experiments are shown as Fig. 12. The reduction of Stanton number with blowing is apparent. For comparison, the laminar solid wall Stanton number under the same conditions occurs at a Stanton number ratio approximately 0.3. When either air or helium is used as an injection coolant, the Stanton number is strongly reduced, and these reductions are found to be in qualitative agreement with the film theory (Ref. 1 and Appendix A) and in rather good agreement with the more complete theory of Ref. 2. The Stanton numbers presented are average values of local Stanton number over the central five inch segment of the seven inch strip, because of the preference to use average recovery factors.

DISCUSSION OF ERRORS

The incompressible turbulent boundary layer theory of Rubesin[5] was used to obtain a qualitative estimate of the effect of variable surface temperature. Calculations showed that the experimental temperature distributions produce local heat-transfer coefficients 8 percent higher than would exist under constant surface temperature conditions.

The data has not been corrected for heat conduction along the surface or across the boundaries of the porous plate. The uncertainty of the heat conduction error varies with mass flow since it is a fixed absolute error.

Measurement of electrical energy input. The measurement of local power dissipations was determined by measuring the voltage differences between two thermocouple locations with a vacuum tube voltmeter. The uncertainty in voltage increments is ± 1 percent. Surface currents were measured by AC ameter to within uncertainties of ± 1/4 percent.

Measurement of local mass flow ratios. The uncertainties in local mass ratios is dependent mainly upon the calibration of the sonic throat areas. Those areas are known to within ± 1 percent. This term causes very little error in the calculation of heat transfer coefficient if temperature difference between the surface and the coolant is small.

Other possible errors. The local Mach number is known to within ± 1 percent. Surface emissivities contain uncertainties of ± 1 percent. The tunnel Reynolds number per inch was held to within ± 2 percent. The above experimental accuracies of quantities computed from the measured data were calculated from the equations for the total differentials.

Error calculations show the uncertainty in the determination of Stanton number increases with injection rate without changing sign. Since

$$\frac{d\,\frac{St}{St_o}}{\frac{St}{St_o}} = \frac{d\,(St)}{St} - \frac{d\,(St_o)}{St_o} ,$$

the increasing departure of the air experimental points from the theory at the high injection rates (Fig. 12) is felt to be due to the onset of larger experimental inaccuracies.

CONCLUSIONS

These heat transfer measurements show that strong mass transfer cooling effects in a turbulent boundary layer are possible at $M = 3.0$, $R_x \approx 4 \times 10^6$, and $T_w/T_\infty = 3.3$ even reducing heat transfer coefficients below laminar values at the higher blowing velocities.

Recovery factors based on temperature have been shown to be reducible by 30 percent with an injection of as little helium as 0.2% of free stream mass flow. The heat transfer coefficient is reduced by over 90% for these same conditions.

Noteworthy is the fact that the limit of relative coolant rates, air to helium, required to effect a given relative Stanton number reduction, as that reduction vanishes, is about 5 which is also the inverse ratio of their specific heats, but that this ratio appears to diminish with increased blowing.

These tests are preliminary to porous cone studies.

APPENDIX A

EXTENSION OF FILM THEORY TO DIFFUSION CASES WHERE THE FRACTIONAL CONCENTRATION OF FOREIGN GAS AT THE WALL DIFFERS FROM UNITY

A correction to the film theory presented in Reference 1 appears to be necessary when the fractional concentration of the foreign gas at the porous wall differs from unity. The dimensionless variables are redefined here in nearly the same form and the results are interpreted for the present application.

The set of differential equations which apply after the consequences of certain simplifying assumptions have been taken into consideration are the following:

$$\frac{\partial}{\partial y}(\rho_i v_i) = 0$$

$$\rho v \frac{\partial u}{\partial y} = \mu \frac{\partial^2 u}{\partial y^2}$$

$$\rho v C_p \frac{\partial T}{\partial y} = k \frac{\partial^2 T}{\partial y^2}$$

$$\rho v \frac{\partial w}{\partial y} = \rho D_{12} \frac{\partial^2 w}{\partial y^2}$$

These equations come from more exact equations which express the conservation of each component of fluid, of momentum, of energy, and of component mass fraction, respectively, upon assuming that any variations in the

stream direction, statistical unsteadiness of the flow, radiation, property value variations, thermal diffusion, internal dissipation and gravitational forces are all negligible.

The last three equations are all of the form

$$\Gamma \frac{d\beta}{dm} = \frac{d^2\beta}{dm^2}$$

satisfying boundary conditions:

$$\beta = 0 \quad \text{at} \quad m = 0$$

$$\beta = 1 \quad \text{at} \quad m = 1 ,$$

if

$$\beta_F = u/u_\infty$$

$$\beta_H = (T_w - T)/(T_w - T_\infty)$$

$$\beta_D = (\omega_w - \omega)/\omega_w$$

and

$$\Gamma_F = \Delta_F \rho v/\mu$$

$$\Gamma_H = \Delta_H \rho v \; Cp/k$$

$$\Gamma_D = \Delta_D \; v/D_{12}$$

$$m = y/\Delta$$

where Δ is the corresponding film thickness.

The solution is

$$\beta = (e^{\Gamma m} - 1)/(e^{\Gamma} - 1)$$

In the limit as the blowing rate goes to zero

$$\beta \rightarrow \beta_{*} = m \quad ,$$

and consequently the limiting boundary layer for zero blowing has linear β variations since

$$\frac{d\beta_{*}}{dy} = \frac{1}{\Delta_{*}}$$

The last equation allows evaluation of Δ_{*} but there is no direct expression which can be written for Δ itself. The assumption is made that blowing does not change the film thickness

$$\Delta \equiv \Delta_{*} \quad .$$

Transfer coefficients at the wall are of practical interest, and in particular their values with blowing relative to their solid wall values are given by

$$\theta_F = \mu_{*_o} c_f / \mu_o c_{f_*}$$

$$\theta_H = k_{*_o} h / k_o h_{*}$$

and a similar parameter for mass transfer which has little meaning. Noting that

$$\theta = \left(\frac{d\beta}{dy}\right)_o \Big/ \left(\frac{d\beta}{dy}\right)_{*o}$$

an alternate expression is readily found

$$\theta = \frac{\Gamma}{e^{\Gamma} - 1} \quad .$$

The heat transfer case is of principal interest here. Stanton number is defined in terms of free stream values

$$St = h/(\rho\ u\ Cp)_{\infty}$$

and

$$\frac{d\phi_*}{dy} = -h_*/k_*(T_w - T_\infty)$$

which permits writing a final expression

$$\frac{St}{St_*} = \frac{(\rho v)_w Cp_w}{(\rho u)_\infty Cp_\infty\ St_*} \Bigg/ \left[\exp\left(\frac{(\rho v)_w Cp_w\ k_{*w}}{(\rho u)_\infty Cp_\infty\ k_w\ St_*} \right) - 1 \right] .$$

It should be noted that the derivation only required that ρv, Cp and k be constant with respect to x and y. It did not require invariance under changes of blowing rate, so k and k_* are not assumed to be equal in the derivation. However, use of $k_{*w}/k_w = k_\infty/k_w$ gave impossible answers so k_{*w}/k_w was set equal to unity. Neither is an evaluation point assigned at which to compute the values of the constants. The subscripts w above are chosen here arbitrarily.

The significant difference between this result and that of Reference 1 is the separation of the quantities ρv and Cp. Thus they may be evaluated from separate considerations, and here the latter is evaluated in the mixed gas at the wall for assumed concnetrations.

It is further assumed that the velocity of the air component is zero at the wall. Therefore,

$$(\rho v)_w = (\rho_1 v_1)_w$$

and one uses simply the mass influx of pure coolant gas.

Calculations have been made for helium assuming $\omega_w = 1$ and $\omega_w = 1/2$ (these are denoted C = 1 and C = 1/2 on Fig. 12), and also for pure air. Use was made of the following formula from Reference 6:

$$Cp_w/Cp_\infty = 1 + 4.1804\,\omega_w$$

REFERENCES

1. Mickley, H.S., Ross, R.C., Squyers, A.L., and Stewart, W.S., Heat, Mass, and Momentum Transfer for flow over a Flat Plate with Blowing or Suction, NACA TN 3208, July 1954.
2. Rubesin, M.W., An Analytical Estimation of the Effect of Transpiration Cooling on the Heat Transfer and Skin Friction Characteristics of a Compressible Turbulent Boundary Layer Skin Friction and Heat Transfer, J.Ae.S., 21, 6, (1954).
3. Dorrance, W.H., and Dore, F.J., The Effect of Mass Transfer on the Compressible Turbulent Boundary Layer Skin Friction and Heat Transfer, J.Ae.S., 21, 6,(1954).
4. Dorrance, W.H., An Addendum, Readers Forum, J.Ae.S., 23, 3, (1956).
5. Rubesin, M.W., The Effect of an Arbitrary Surface Temperature Variation Along a Flat Plate on the Convective Heat Transfer in an Incompressible Turbulent Boundary Layer, NACA TN 2345, April 1951.
6. Hirschfelder, J.D., Curtis, C.T., and Bird, R.B., Molecular Theory of Gases and Liquids, John Wiley and Sons, New York, 1954.

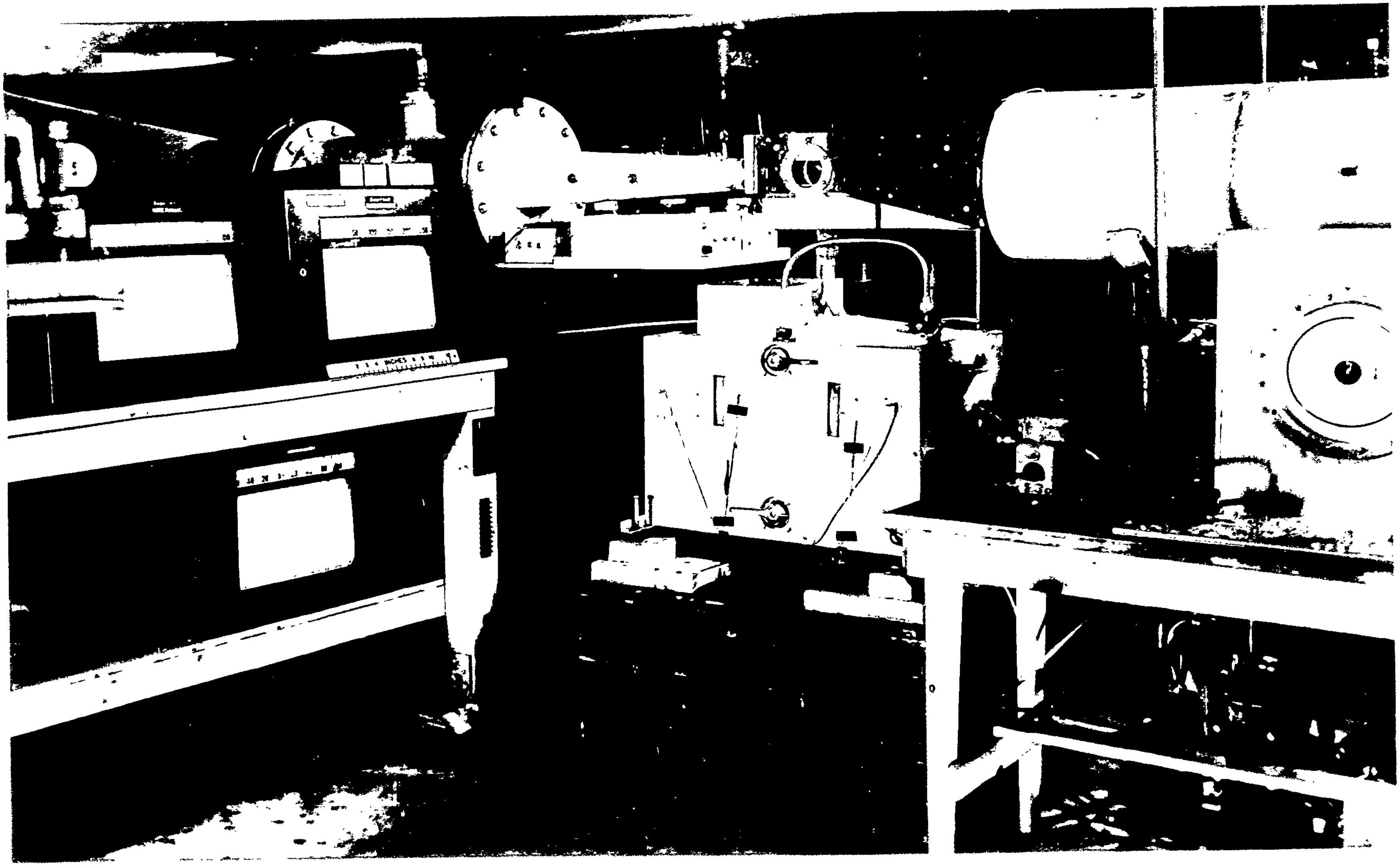

Figure 1. View of Mach number 3 instrumentation channel and associated instrumentation.

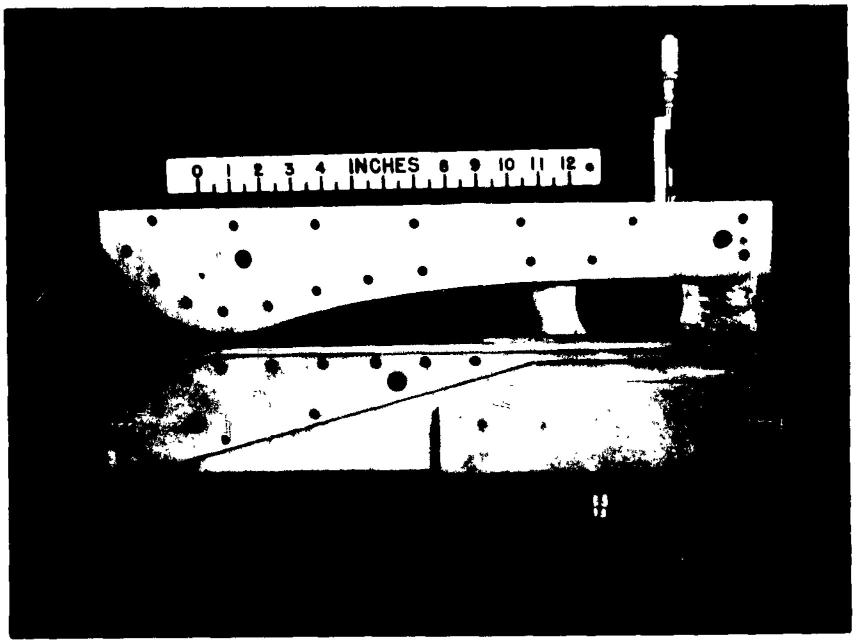

Figure 2. The Mach number 3 test section showing position of porous surface.

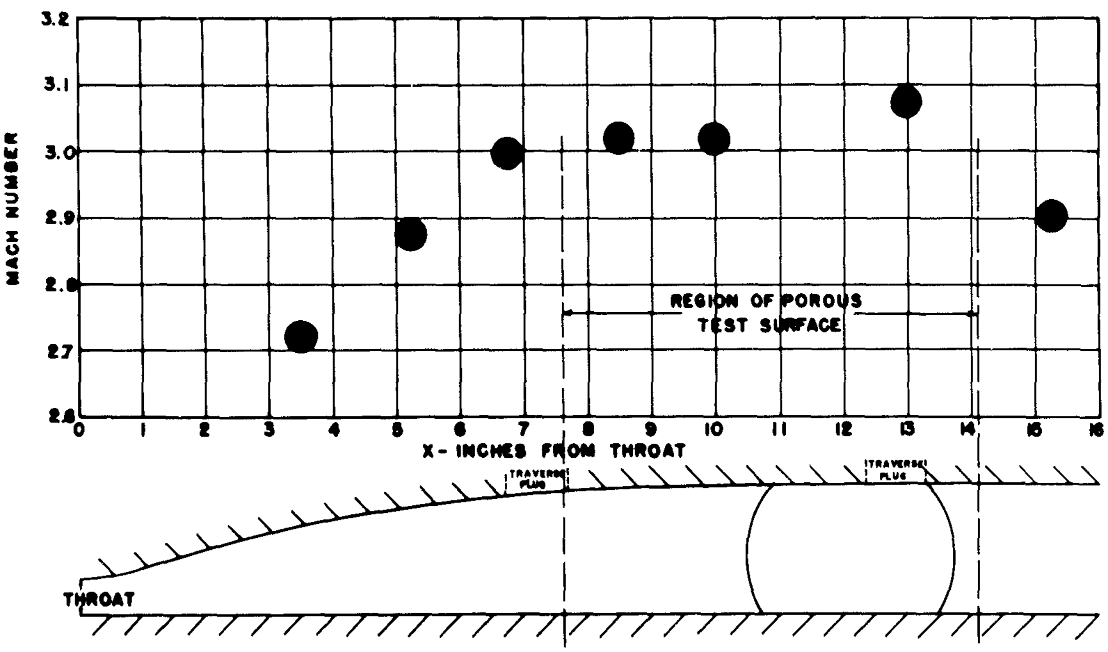

Figure 3. Mach number distribution along straight wall of instrumentation channel.

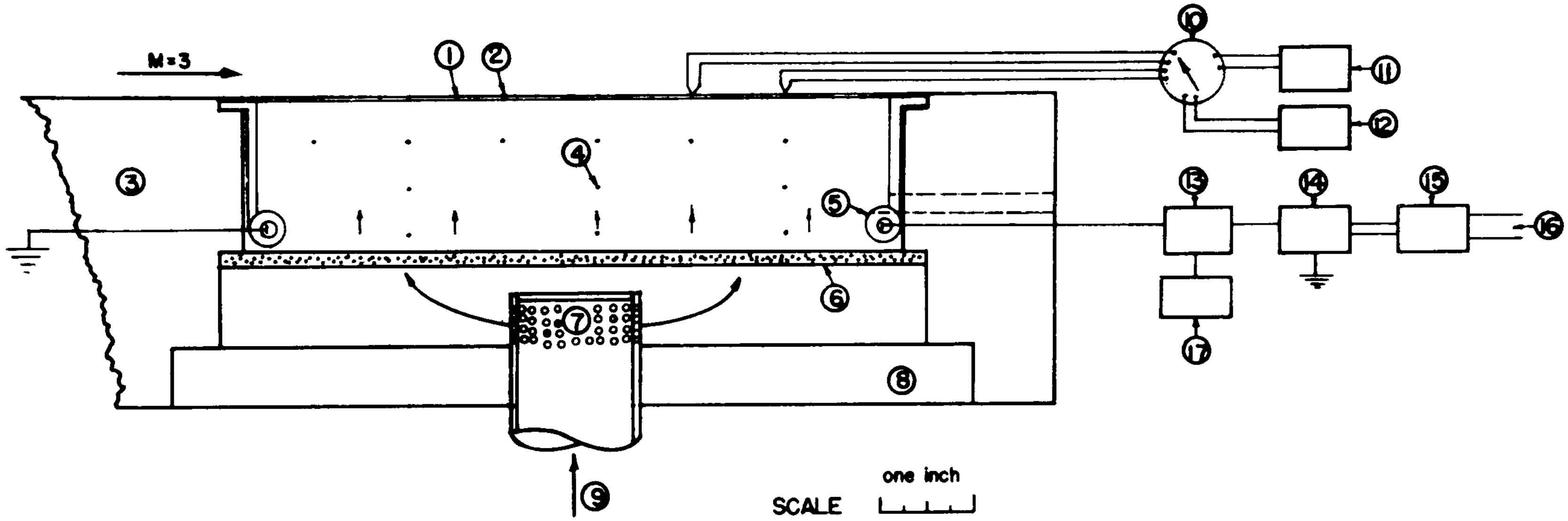

① POROUS SURFACE (POROLOY)
② SURFACE THERMOCOUPLE — T_w
③ NOZZLE BLOCK (SCOTCHPLY)
④ COOLANT THERMOCOUPLE — T_c
⑤ COPPER BUS BAR
⑥ POROUS BRONZE BAFFLE
⑦ COOLANT INTAKE BAFFLE
⑧ COVER PLATE
⑨ COOLANT SUPPLY PIPE
⑩ SELECTOR SWITCH
⑪ TEMPERATURE RECORDER
⑫ VACUUM TUBE VOLTMETER
⑬ CURRENT TRANSFORMER
⑭ POWER TRANSFORMER
⑮ VOLTAGE REGULATOR
⑯ 115-VOLT A.C. LINE
⑰ AMMETER A.C. RMS

Figure 4. Flow pattern, instrumentation, and wiring diagram for the electrically heated porous surface.

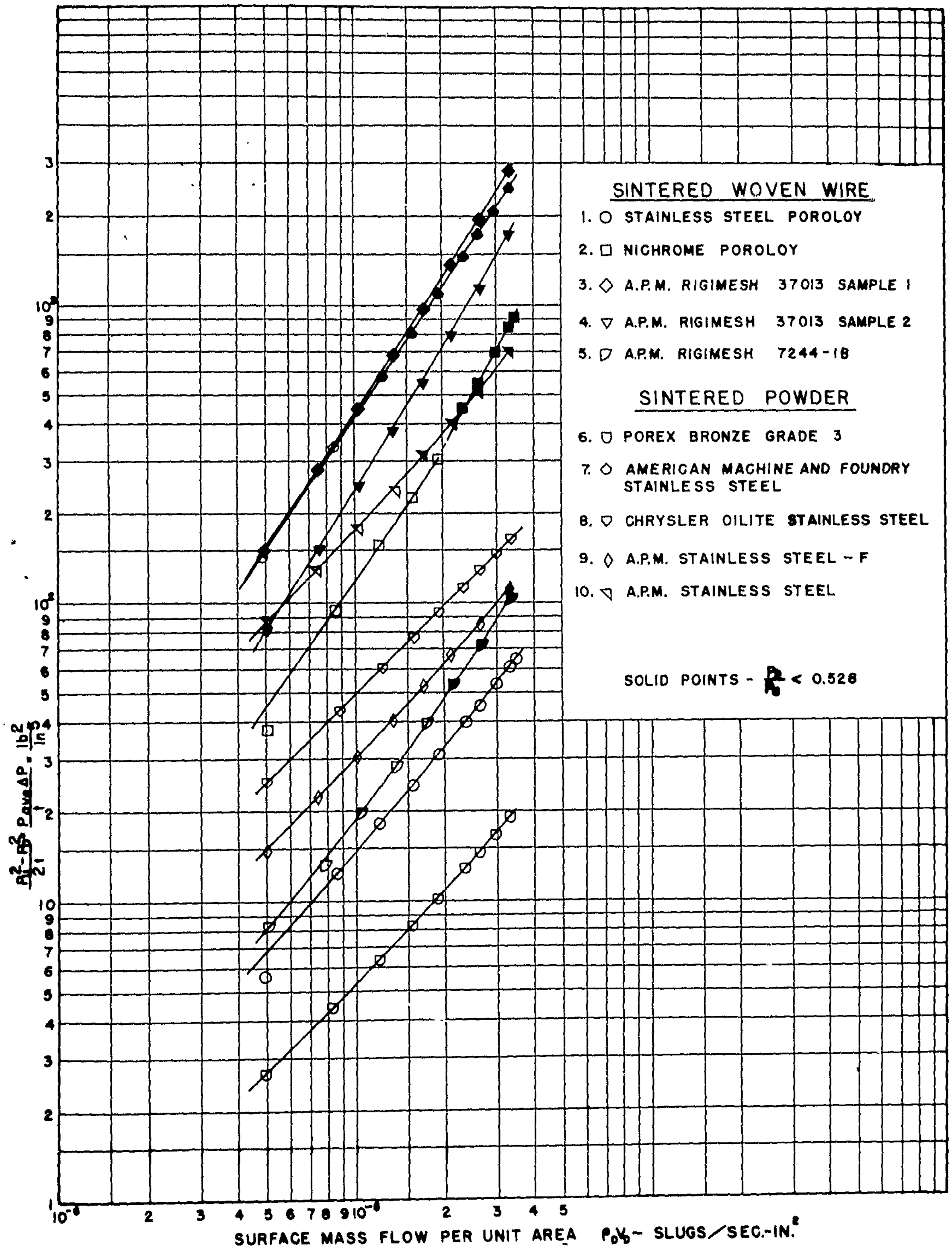

Figure 5. Permeability parameter $P_{ave} \Delta P/t$ vs. air mass flow per unit area for several porous materials.

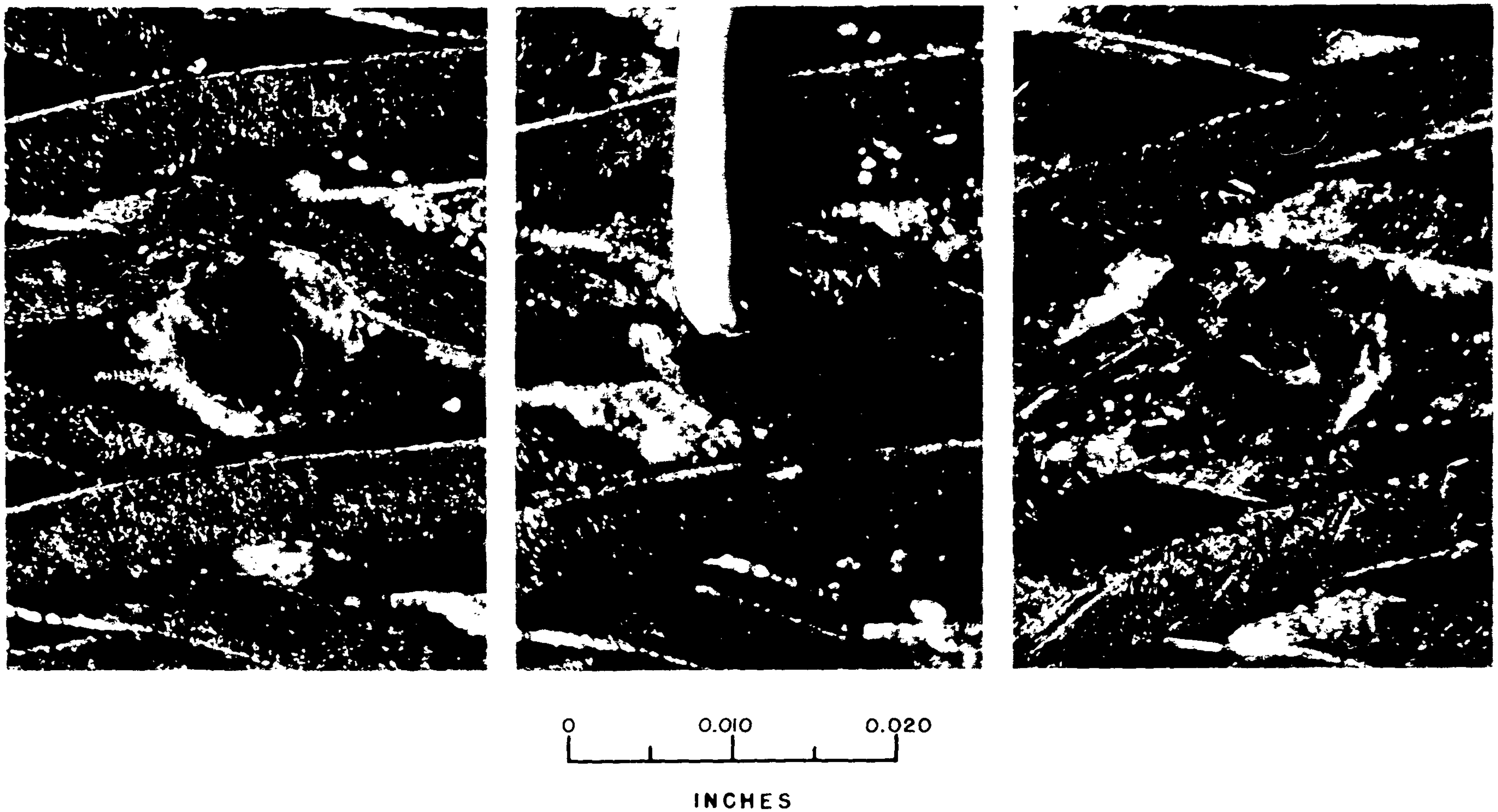

Figure 6. Installation of .0031 in. diam. thermocouple wires. Teflon plug, wires inserted, wires cut and welded to sintered wire surface.

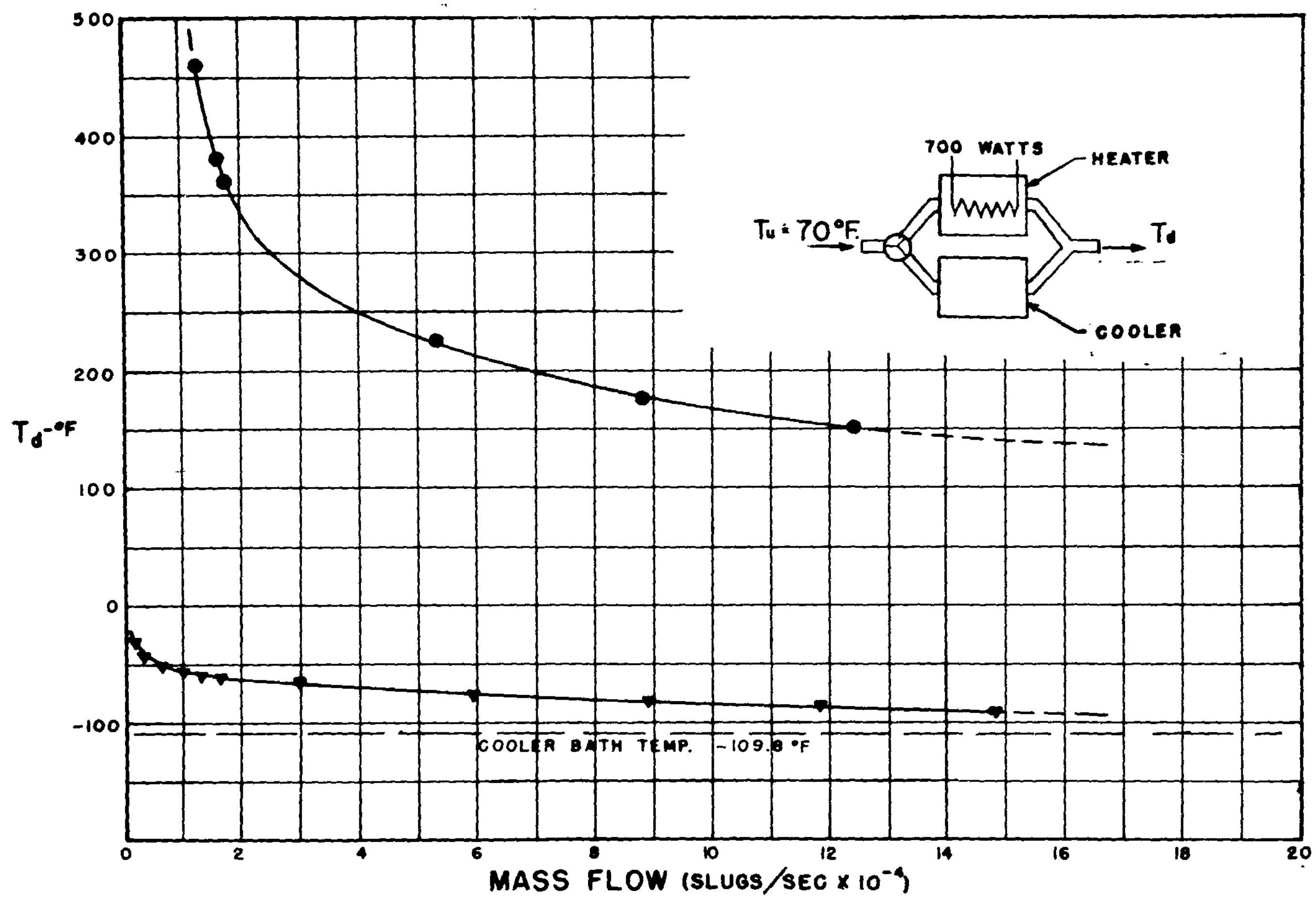

Figure 7. Performance envelope of heater-cooler combination.

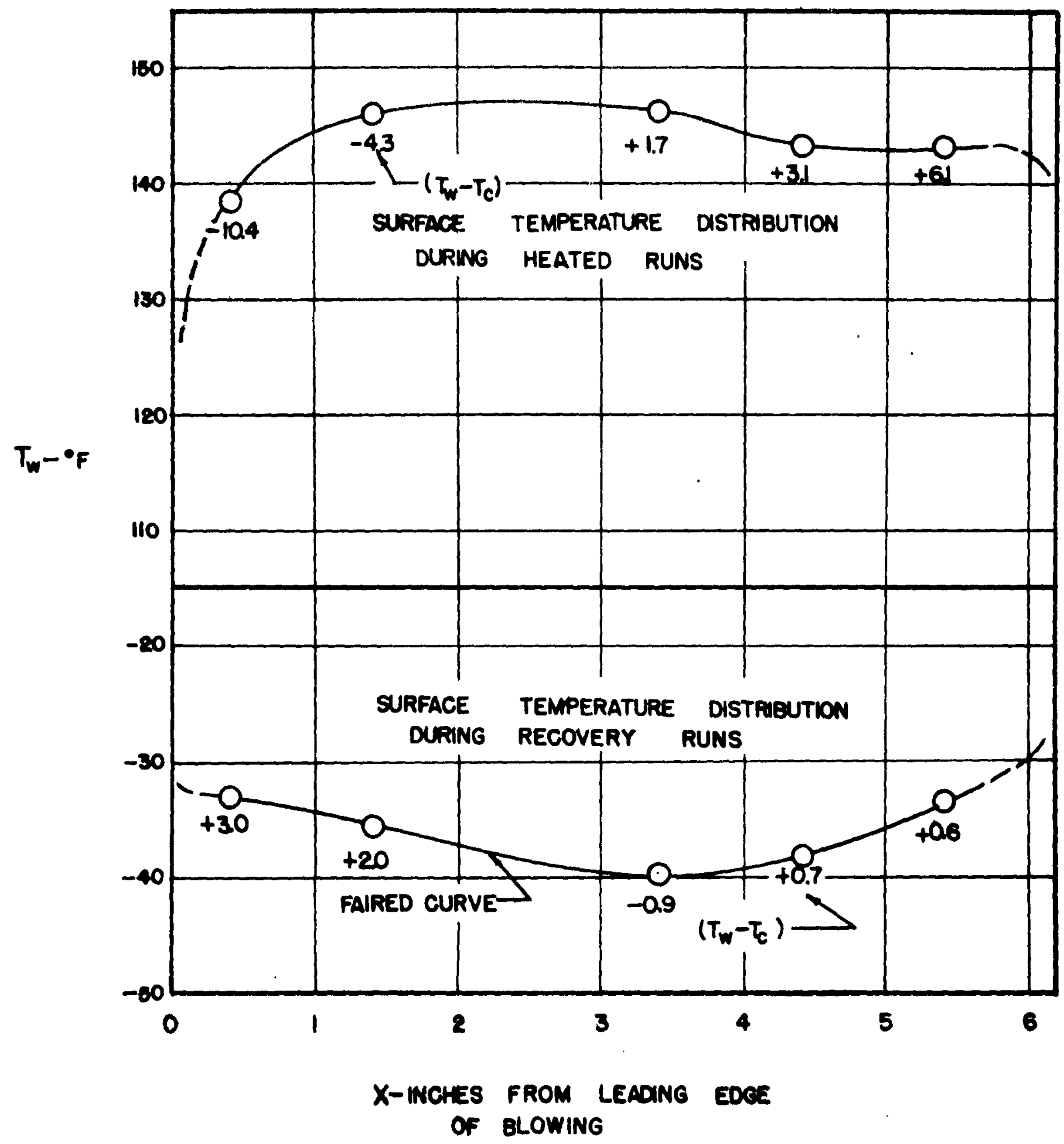

Figure 8. Typical surface temperature distributions measured during heated and recovery runs. Local values of T_w-T_c are listed for each thermocouple set.

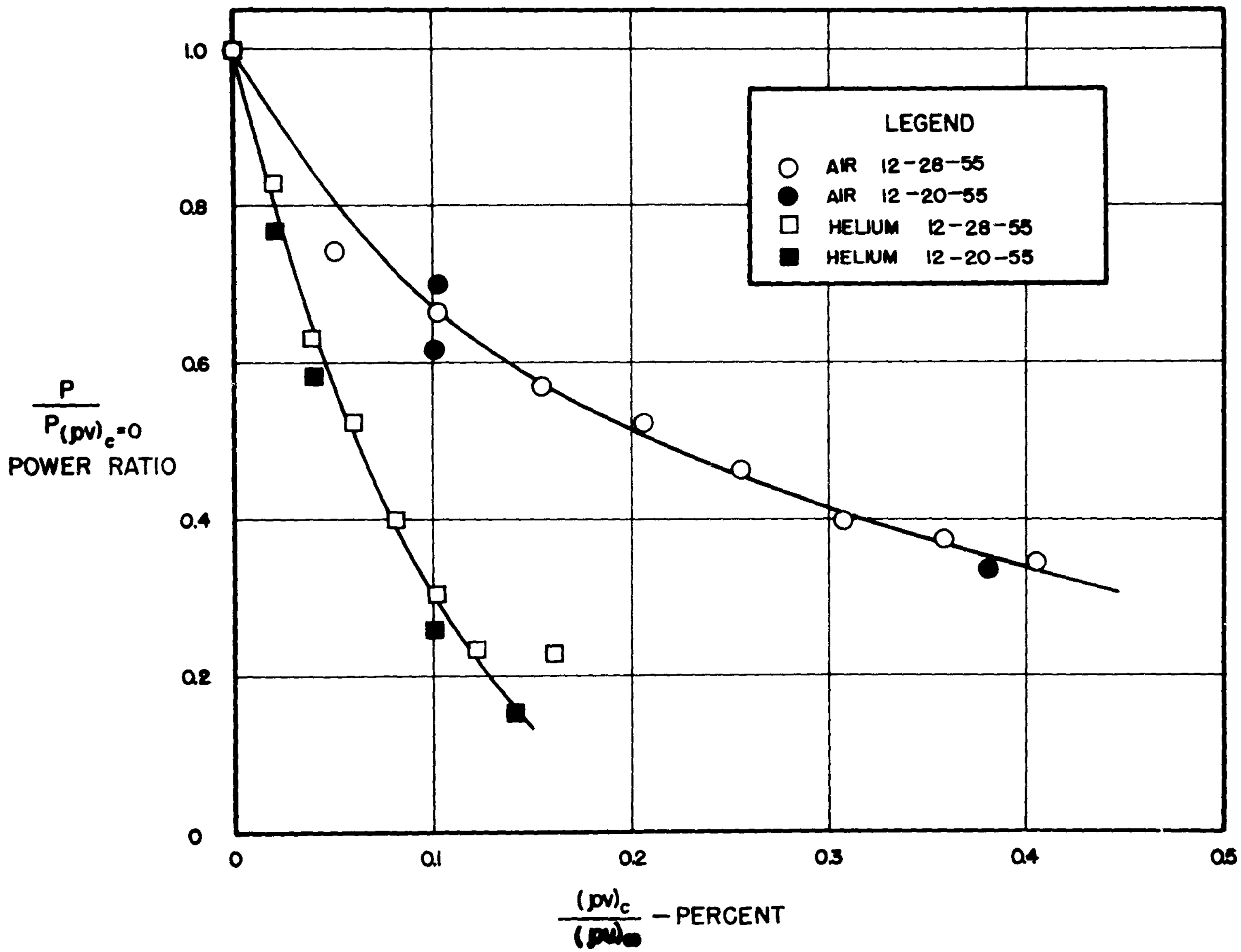

Figure 9. Power required to maintain $T_s = 135^{\circ}F$ with injection of air and helium.

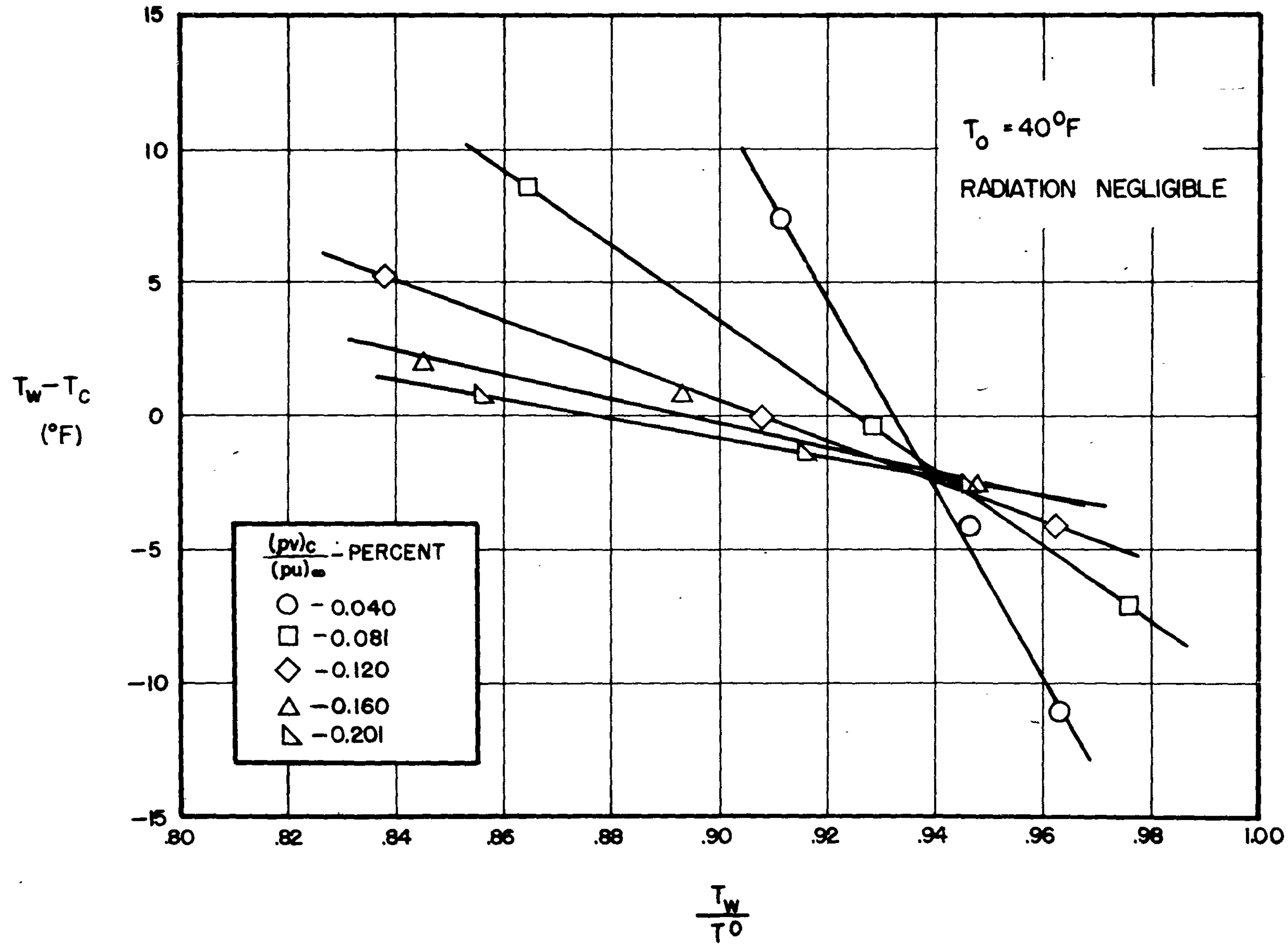

Figure 10. Interpolation of local recovery temperature ratio from local wall and coolant temperatures. Helium injection.

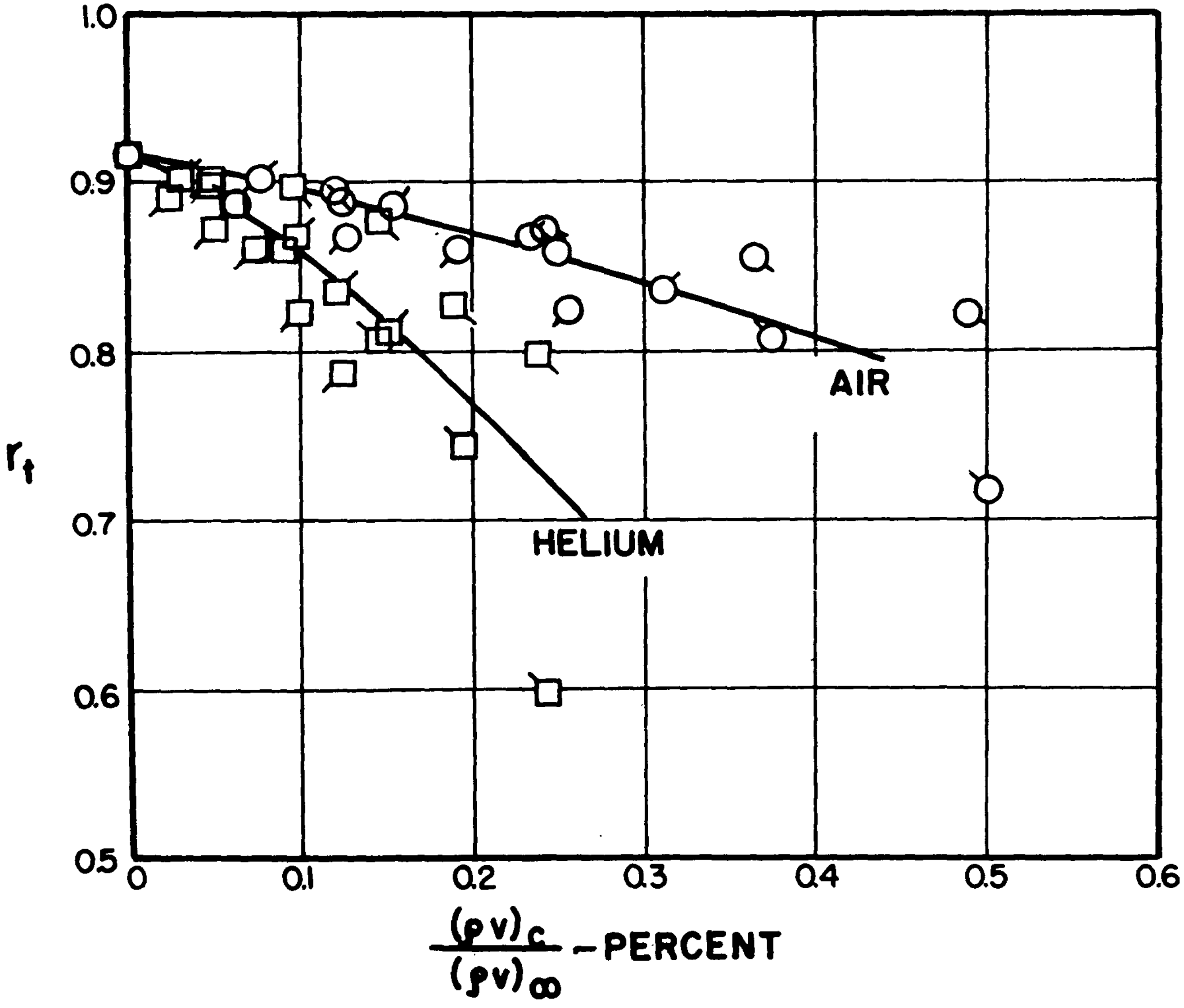

Figure 11. Variation of temperature recovery factor with injection of helium and air. (Note - flagged points indicate individual thermocouple sets.) $r_{t_o} = .9127$.

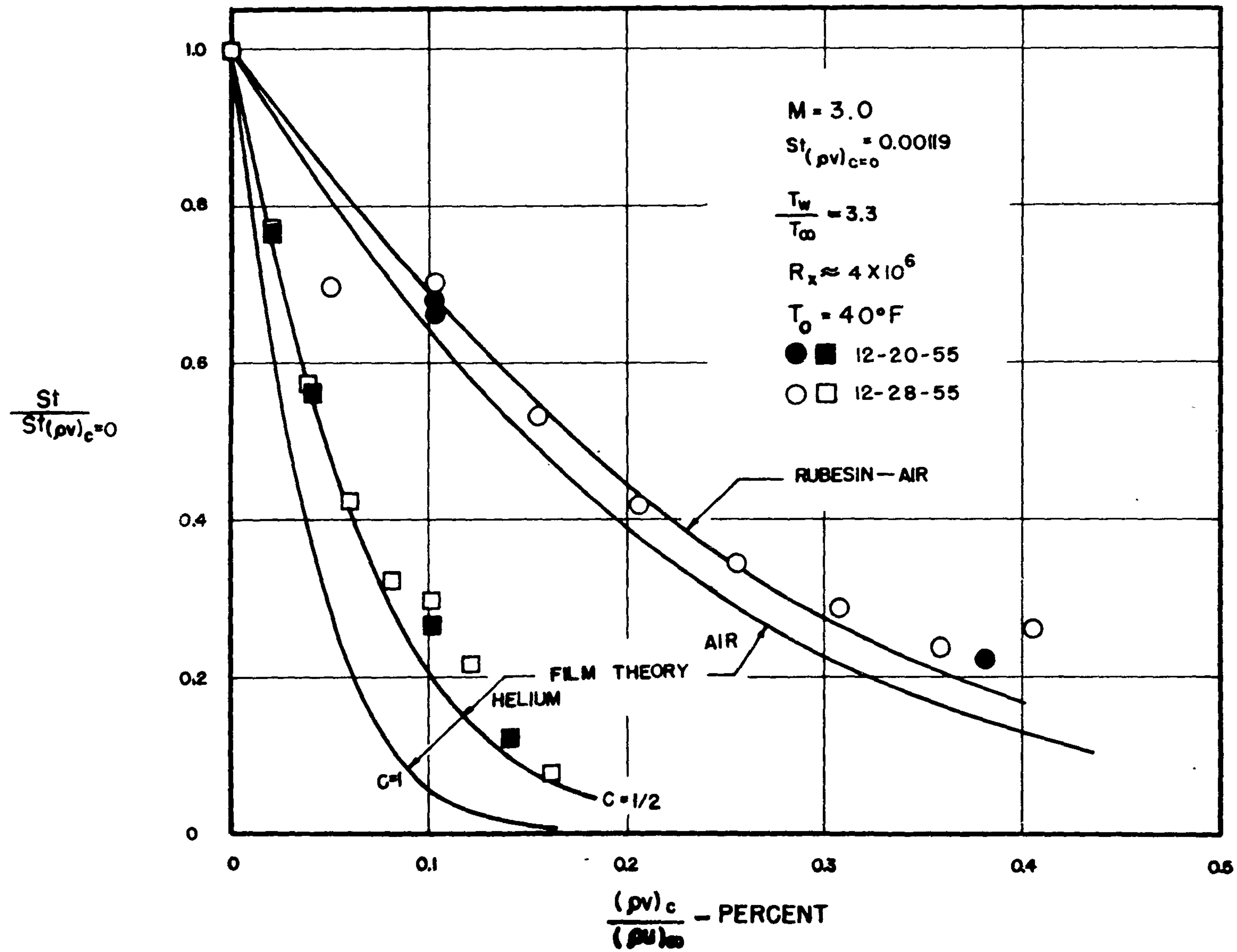

Figure 12. Comparison of measured turbulent Stanton numbers with available theories.

DISTRIBUTION LIST

1.	Office of the Secretary of Defense Washington 25, D. C.	1
2.	Chief, Document Service Center Dayton 2, Ohio	5
3.	Commander, Air Res. and Development Command Baltimore 3, Maryland	1
4.	Chief, European Office Washington 25, D. C.	2
5.	Commander, Arnold Engineering Development Center Tullahoma, Tennessee	1
6.	Commander, Wright Air Development Center Wright-Patterson Air Force Base, Ohio	2
7.	Commander, Western Development Division Inglewood, California	1
8.	Commander Air Force Cambridge Research Center Cambridge 39, Massachusetts	1
9.	Commander, Holloman Air Development Center Alamorgordo, New Mexico	1
10.	Chief of Staff, U.S. Air Force Washington 25, D. C.	1
11.	Commander Air Research and Development Command Baltimore 3, Maryland	3
12.	Chief, Western Division Pasadena 2, California	1
13.	Commander, Air Force Missile Test Center Cocoa, Florida	1
14.	Commander, Maxwell Air Force Base Alabama	1
15.	Director, U.S. Naval Research Laboratory Washington 25, D. C.	1
16.	Chief, Bureau of Aeronautics Washington 25, D. C.	1
17.	Commander, Naval Air Development Station Johnsville, Pennsylvania	1
18.	Chief, Bureau of Ordnance, Dept. of Navy Washington 25, D. C.	1

19.	Commander, Naval Ordnance Test Station China Lake, California	1
20.	Commander, Taylor Model Basin Carderock, Maryland	1
21.	Chief of Naval Research Washington 25, D. C.	1
22.	Commander, Naval Ordnance Laboratory Silver Spring, Maryland	1
23.	Chief, Bureau of Ships Washington 25, D. C.	1
24.	Office of the Chief of Ordnance Washington 25, D. C.	1
25.	Director Ballistics Research Laboratory Aberdeen, Maryland	1
26.	Commanding Officer, Office of Ordnance Research Duke Station, Durham, North Carolina	1
27.	Atomic Energy Commission Washington 25, D. C.	1
28.	Director, Ames Aero Lab., NACA Moffett Field, California	1
29.	Director, Aero Research, NACA Washington 25, D. C.	1
30.	Director, Langley Memorial Aero Lab., NACA Langley Field, Virginia	1
31.	Director, Lewis Flight Lab., NACA Cleveland, Ohio	1
32.	National Bureau of Standards Washington 25, D. C.	1
33.	National Science Foundation Washington 25, D. C.	1
34.	Department of Aero. Eng. and Appl. Mech. Polytechnic Institute of Brooklyn	1
35.	Guggenheim Aeronautical Laboratory Pasadena 4, California	1
36.	Department of Aeronautical Engineering University of Michigan, Ann Arbor	1

37.	Boeing Airplane Company Seattle 14, Washington	1
38.	Consolidated Vultee A/C Corporation San Diego 12, California	1
39.	Curtiss-Wright Corporation Caldwell, New Jersey	1
40.	Douglas Aircraft Co., Inc. Santa Monica, California	1
41.	Bell Aircraft Corporation Buffalo 5, New York	1
42.	Cessna Aircraft Company Wichita 1, Kansas	1
43.	Convair, Fort Worth Division Fort Worth, Texas	1
44.	Douglas Aircraft Company El Sequnde, California	1
45.	Fairchild Engine and Aircraft Company Wyabdanch, Long Island, New York	1
46.	General Electric Company West Lynn, Massachusetts	1
47.	Gruman Aircraft Engineering Corporation Bethpage, Long Island, New York	1
48.	General Electric Company Schenectady, New York	1
49.	The Glenn L. Martin Company Baltimore 3, Maryland	1
50.	Goodyear Aircraft Corporation Akron, Ohio	1
51.	Hughes Aircraft Company Culver City, California	1
52.	Lockheed Aircraft Corporation Burbank, California	1
53.	McDonnel Aircraft Corporation St. Louis 3, Missouri	1
54.	Marquardt Aircraft Corporation Van Nuys, California	1

55.	Northrop Aircraft, Inc. Hawthorne, California	1
56.	Reaction Motors, Inc. Rockaway, New Jersey	1
57.	The Rand Corporation Santa Moniça, California	1
58.	Republic Avaiation Corporation Farmingdale, Long Island, New York	1
59.	United Aircraft Corporation East Hartford 8, Connecticut	1
60.	Westinghouse Electric Corporation Philadelphia 13, Pennsylvania	1
61.	Library, University of Texas Austin, Texas	1
62.	Aero. Eng. Library, Forrestal Research Center Princeton, New Jersey	1
63.	Library, Mass. Inst. of Technology Cambridge 39, Massachusetts	1
64.	John Crevar Library Chicago 1, Illinois	1
65.	Applied Mechanics Reviews Kansas City 2, Missouri	2
66.	Aeronautical Engineering Reviews New York 21, New York	2
67.	Library, Calif. Inst. of Technology Pasadena 4, California	1
68.	Commander, Air Material Command Wright-Patterson Air Force Base, Ohio	1
69.	Applied Physics Lab., Johns Hopkins University Silver Spring, Maryland	1
70.	Director, High Speed Flight Res. Station Edwards Air Force Base, California	1
71.	Jet Propulsion Laboratory, Calif. Inst. of Tech. Pasadena 3, California	
72.	Cornell Aeronautical Laboratory Buffalo 21, New York	1

73. Defense Res. Lab., University of Texas
Austin, Texas 1

74. Dr. J. Kaye, Dept. of Mechanical Engineering
Massachusetts Institute of Technology, Cambridge 1

75. Forrestal Research Center, Princeton University
Princeton, New Jersey 1

76. Aerojet Engineering Corporation
Azusa, California 1

77. The Ramo-Woolridge Corporation
Los Angeles 45, California 1

78. Jackson R. Stolder, Ames Aeronautical Laboratory
Moffett Field, Los Angeles, California 1

79. Professor N. A. Hall, College of Engineering
University Heights, New York 53, New York 1

80. De. C. Desmond Pengelley, Southwest Res. Inst.
San Antonio 6, Texas 1